Computer Aided Innovation of New Materials
M. Doyama, T. Suzuki, J. Kihara and R. Yamamoto (Editors)
Elsevier Science Publishers B.V. (North-Holland), 1991

Simulation of ULSI Processes and Devices

Hans KOSINA, Karl WIMMER, Claus FISCHER, Siegfried SELBERHERR

Institut für Mikroelektronik, Technische Universität Wien,
Gußhausstraße 27-29, A-1040 Wien, Austria

Devices with feature sizes less than a micrometer are required for monolithic ULSI circuits. These devices can only be efficiently developed with the aid of computer simulation. This contribution is intended to review the state of the art in process and device simulation for these ULSI devices.

1 Introduction

Simulation has become indispensable for the development and redesign of devices in the area of ULSI.

Process simulation is necessary to understand the impact of successive process steps on doping distribution and wafer topography. We intend to review the state of the art in modeling ion-implantation, annealing, diffusion and thermal oxidation.

As to *device simulation*, the physical assumptions which are required to describe carrier transport are discussed. Particular emphasis is put on the extension of the classical drift-diffusion approach in order to meet accurately the requirements of ULSI device analysis.

2 Process Simulation

The device fabrication processes can in principle be categorized into two groups. Lithographic processes which build up the wafer topography, and doping processes which determine the electrical properties of the intended device for a given structure. The first group consists of deposition and etching with spatial selectivity in order to enable structuring. The second group is composed of ion-implantation, annealing, diffusion, thermal oxidation and epitaxy.

2.1 Ion-Implantation

Ion-implantation has developed into the most important doping technique for integrated circuits.

To describe ion-implantation profiles methods based on distribution functions together with spatial moments have been used widely in the last two decades. In principle these methods assume a functional type for the distribution function and calculate its free parameters from its spatial moments. The spatial moments may be obtained either by experiments [57] or by theory [20, 36, 79].

The above sketched methods are based on point-responses in (semi-)infinite targets [56] and suffer in accuracy for complex targets [58]. As a review on these problems [59, 68] can be recommended.

To overcome these drawbacks more sophisticated models based on Boltzmann transport equations [21, 70] or Monte Carlo simulation [9, 38] have to be applied. The Monte Carlo method can be extended to the simulation of recoil cascades and defect production [25, 28, 74]. Recently major efforts have succeeded in increasing computational efficiency [25, 26, 62].

Present investigations focus on channeling effects in order to explain the deeper penetration of ions implanted in channeling direction [27, 39, 44]. It has been shown that the electronic stopping power is significantly reduced for channeled ions. In Fig. 1 a profile of boron implanted in channeling direction is compared with simulations [27]. It shows that the experimental data can only be reproduced by simulations using a model for the electronic stopping power which depends on the impact parameter (Oen-Robinson [46]).

2.2 Diffusion

Diffusion is the physical mechanism which is responsible for the redistribution of impurity atoms. As a review on this problem [5] can be recommended. The diffusion of dopants is assumed to follow the two laws of Fick.

$$\mathbf{J} = -D \cdot \left(\operatorname{grad} C_t - z \cdot \frac{q}{k\,T} \cdot C_a \cdot \operatorname{grad} \psi \right) \qquad (1)$$

$$\frac{\partial C_t}{\partial t} + \operatorname{div} \mathbf{J} = 0 \qquad (2)$$

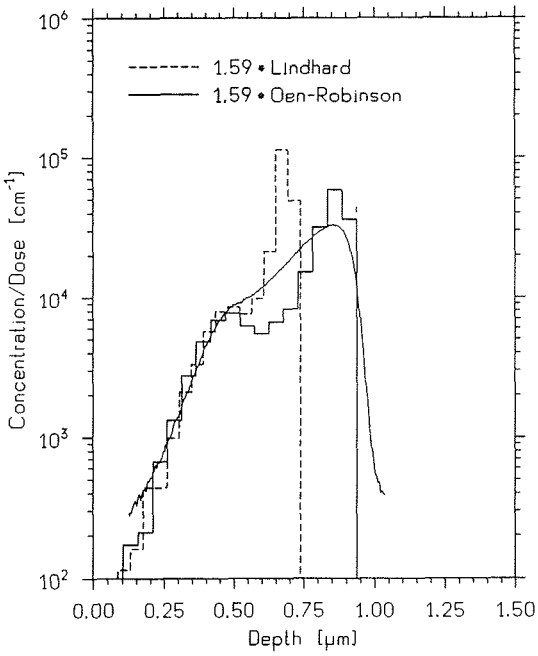

Fig. 1: Boron implanted in <111> Si, 150 keV, in channeling direction

For any dopant C_t is the total concentration, C_a is the electrically active part of the concentration, z is the charge state, and ψ the electrostatic potential.

Up to now, the determination of the nature of the effective diffusivity D has accounted for most of the work in modeling. It is commonly assumed that dopants in silicon diffuse by interaction with point defects (vacancies, interstitials) in various charge states [13].

The first well-established model has been proposed by Fair [17]. The diffusion via vacancies in each charge state is proportional to the concentration of the respective vacancy species.

$$D = D^o + D^- C_V^- + D^= C_V^= + D^+ C_V^+ \qquad (3)$$

The existence of vacancies of just four charge states (neutral o, single negative $-$, double negative $=$ and positive $+$) has been shown by Watkins [78]. The temperature dependencies of the individual diffusivities in (3) are modeled with Arrhenius laws. The normalized vacancy concentrations can be obtained by a simple mass action law [66].

Basically, the electrostatic potential ψ is to be obtained by solving the Poisson equation, though in almost all cases the zero space charge approximation can be applied [32].

At high dopant concentrations not all dopant atoms are ionized due to clustering and precipitation. The electrically active part C_a of the concentration must be estimated either by static relations [22] or the solution of appropriate differential equations [32, 75].

Unfortunately Fair's model (3) cannot be applied when anomalous diffusion effects associated with surface injection of defects are considered. Oxidation, nitridation and oxinitridation are all well known to perturb the defect concentrations and therefore the dopant diffusivities [1, 15, 41, 71].

To account better for the point defect concentrations, the diffusion coefficient is usually split into a vacancy and an interstitial contribution in the form [4]

$$D = D_i \cdot \left(f_i \cdot \frac{C_I}{C_I^{eq}} + (1 - f_i) \cdot \frac{C_V}{C_V^{eq}} \right) \qquad (4)$$

with the diffusivity under inert and intrinsic conditions D_i, and the interstitial and vacancy concentrations C_I and C_V, respectively. The factor f_i characterizes the contribution of interstitials to the diffusivity. The superscript eq denotes equilibrium conditions. The interstitial and vacancy concentration can be achieved by solving standard continuity equations.

$$\frac{\partial C_I}{\partial t} = \mathrm{div}(D_I \,\mathrm{grad}\, C_I) - k_b \cdot (C_I C_V - C_I^{eq} C_V^{eq}) \qquad (5)$$

$$\frac{\partial C_V}{\partial t} = \mathrm{div}(D_V \,\mathrm{grad}\, C_V) - k_b \cdot (C_I C_V - C_I^{eq} C_V^{eq}) \qquad (6)$$

D_I, D_V, and k_b are the diffusivities for interstitials and vacancies, and the bulk reaction constant, respectively. The reported values for the diffusivities and the equilibrium concentrations cover a range of several orders of magnitude [11, 71, 72], and there are many open questions regarding the bulk reaction constant and the formulation of the boundary conditions [35].

Certain anomalous diffusion effects, such as the kink in phosphorus profiles and the enhanced tail diffusion in boron and phosphorus profiles become more pronounced at low temperatures [16, 48]. As an example Fig. 2 shows the simulation of phosphorus diffusion [51]. During rapid thermal processing [40], a transient diffusion enhancement has been reported. The recent approaches in modeling these effects are based on point defect and pair formation kinetics. Related simulations use a pair-diffusion model, consisting of 5 equations for interstitials, vacancies, substitutional dopants, dopant-interstitial pairs, and dopant-vacancy pairs.

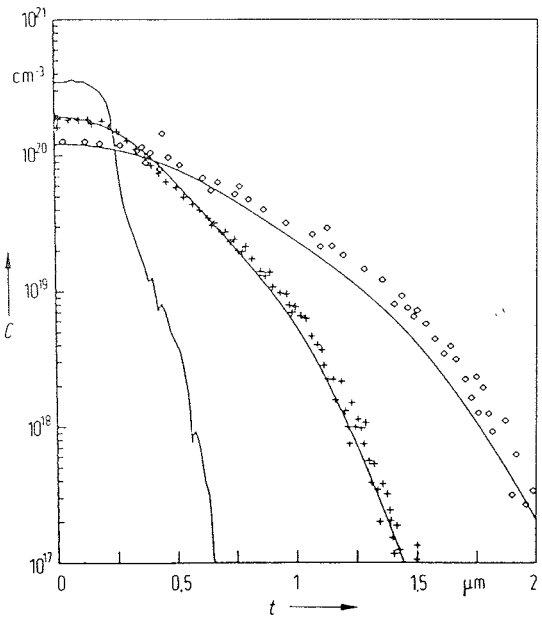

Fig. 2: Simulation of phosphorus diffusion at 1000°C compared to experimental data (+ 60 min, ◇ 250 min)

Although simulations using a pair-diffusion model have been successfully fitted to experimental data [12, 43, 47, 51], further investigations are definitely necessary to determine the numerous parameters in a physically sound manner. New experiments will have to be cleverly designed in order to isolate the various overlapping and compensating effects.

2.3 Oxidation

The oxidation of silicon is a thermal process by which the oxidizing species diffuse through an existing oxide layer and react with the silicon atoms. The chemical reaction is accompanied by a volume expansion (125 % for the Si-SiO_2 complex) so that the existing oxide is forced away by the newly formed oxide layer, and a visco-elastic flow of the oxide film. As a review on the whole subject [42, 52] can be recommended.

The simulation of the growth has been based for many years on the work of Deal and Grove [14]. In their paper they have assumed the fluxes across the ambient/oxide interface, through the oxide and at the oxide/silicon interface to be equal. Thereby one obtains the following relationship for the oxide thickness d_{ox}.

$$d_{ox}^2 + A \cdot d_{ox} = B \cdot (t + t_o) \qquad (7)$$

B and B/A are the parabolic and linear oxidation rate, respectively. t_o accounts for an eventually existing initial oxide. This formula is well suited to describe the oxide growth for wet oxidation. For dry oxidation deviations from (7) have been observed, and several authors [29, 52, 73] modified (7) to take the rapid initial oxidation into account. Recently some papers [45, 80] have been published, predicting a power law in the form $d_{ox} = a\,t^b$.

For two- and three-dimensional oxidation no well established theory is available today, cf. [33]. The first successful attempt to simulate the lateral oxidation near a mask edge (bird's beak) dates back to Penumalli [49], predicting the oxide shape a-priori in a parametric form. More realistic models for the moving $Si - SiO_2$ interface are based on a steady-state oxidant diffusion, and visco-elastic flow of the oxide [60, 63, 76]. For temperatures above 950°C, incompressible creeping flow equations are commonly used, e.g. [33, 77]. Considerable effort has been spent on analyzing the influence of mechanical stress on the kinetic parameters of oxidation [53, 69], and on models for the interface conditions which describe the point defect generation and recombination [35].

Further studies are evidently needed to clarify in sufficient detail the physics underlying oxidation.

3 Device Simulation

Device Modeling based on the self-consistent solution of the basic semiconductor equations dates back to the famous work of Gummel in 1964 [23]. Since then numerical device modeling has been applied to nearly all important devices. The current relations which are the most complex equations out of the set of the basic semiconductor equations have been frequently subject of discussions, in particular in view of their applicability to submicron devices. Methods how to overcome the limitations of the classical drift diffusion approach will be discussed in the following.

3.1 Drift Diffusion Model

The classical semiconductor equations [64] for the variables (ψ, n, p) consist of Poisson's equation

$$\mathrm{div}(\epsilon \cdot \mathrm{grad}\,\psi) = -\rho \qquad (8)$$

with the space charge $\rho = q \cdot (p - n + N_D^+ - N_A^-)$, and of the carrier continuity equations

$$\mathrm{div}\,\mathbf{J_n} = q \cdot R, \quad \mathrm{div}\,\mathbf{J_p} = -q \cdot R. \qquad (9)$$

The drift-diffusion approximation for the current density utilizes a simplified form of the momentum conservation equation.

$$\mathbf{J_n} = -q\,\mu_n\,n \cdot \left(\text{grad}\,\psi - \frac{1}{n} \cdot \text{grad}\left(\frac{k\,T_n}{q} \cdot n\right)\right) \quad (10)$$

$$\mathbf{J_p} = -q\,\mu_p\,p \cdot \left(\text{grad}\,\psi + \frac{1}{p} \cdot \text{grad}\left(\frac{k\,T_p}{q} \cdot p\right)\right) \quad (11)$$

Commonly it is assumed that the carrier temperatures T_n and T_p are equal to the lattice temperature, and that the gradients of the carrier temperatures are zero. The current relations include the mobilities of electrons and holes, which have to be appropriately modeled to describe correctly the various scattering phenomena. A great variety of scattering mechanisms has to be taken into account. Most important are lattice scattering, ionized impurity scattering, velocity saturation, and surface scattering. A review of many models can be found in [64]; the evolution of one particular model for MOS devices is presented in [65].

3.2 Classical Monte Carlo Method

The principle of the Monte Carlo method as applied to device simulation is to simulate the motion of a carrier in the state space. This motion consists of an alternating sequence of drift in the electric field and scattering events. The drift time of the electron, the type of scattering and the final state are random quantities with probability distributions depending on the underlying semiconductor model. The duration of the free flight is chosen randomly according to the cumulative probability [18]

$$P(t) = 1 - \exp\left(-\int_0^t \lambda(\mathbf{k}(t'), t')dt'\right), \quad (12)$$

where $\lambda(\mathbf{k}, t')$ denotes the total scattering rate, which is the sum of all individual scattering rates. Usually fictitious "self scattering" is introduced to simplify the free flight time calculation [54, 55].

In time invariant simulations the quantities of interest are obtained as steady state averages over the carrier ensemble which can be efficiently calculated by

$$< A(\mathbf{k}) > = \frac{\sum A(\mathbf{k}_{bi})\lambda(\mathbf{k}_{bi})^{-1}}{\sum \lambda(\mathbf{k}_{bi})^{-1}}, \quad (13)$$

where the sum covers all electron free flights; $\mathbf{k}_{bi}$ indicates the wave vector at the end of the free flight immediately before the i-th scattering event [50, 61].

3.3 Quantum effects

When the potential gradients approach very high values, the resulting quantum effects cause differences from the drift diffusion model in both carrier concentration and transport. Surfaces, heterojunctions, and other locations where the physical parameters of the materials change have therefore to be taken into special consideration. Although the influence of these phenomena seems to be drastic at first glance, experience which has been recently gathered proves that many problems with surface and interface effects can be accounted for by simple adaptions of the simulation parameters near the surface.

As for the determination of carrier concentrations in quantum effect devices, such as heterostructures and superlattices, the effective mass approximation is widely used as a basis to the calculation [3].

In equilibrium, the one-electron approximation provides a time-independent Schrödinger equation

$$\left(-\frac{\hbar^2}{2m^*}\Delta + V_{(x,y,z)}\right)\Psi = E_n\Psi \quad (14)$$

which can often be reduced to one dimension.

Since the potential energy $V_{(x,y,z)}$ depends strongly on the carrier concentration, the solution must be achieved self-consistently. Fig. 3 shows as an example the potential energy in the inversion layer of a MODFET together with the first 3 wave functions.

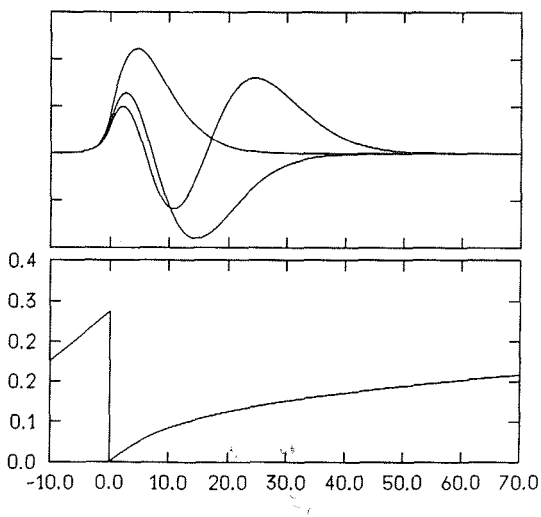

Fig. 3: The first 3 Eigenfunctions of the Schrödinger equation together with the self-consistently calculated potential energy in a MODFET inversion layer (length unit μm, potential energy unit eV, wave function scale unit $10^{-4}\ m^{-0.5}$)

Some methods have been suggested how to consider many-body-effects and image forces easily by including additional terms in the potential energy V [67]. Different types of carriers or different valleys in the energy band structure are sometimes taken into account by solving a system of coupled Schrödinger equations [8].

These methods have been successfully used for the calculations of energy levels and transition energies in optical devices.

As for the transport in quantum well devices, efforts are currently made to couple the wave functions with the classical drift-diffusion approximation or Monte Carlo methods. The aim is to achieve models that are as straightforward and fast to implement as the drift-diffusion approximation and fit the quantum effects with sufficient accuracy.

The deviations between the classical and the quantum-physical solution [81] depend on the density of eigenenergies in the energy scale compared to kT, which decreases when the quantum well width increases, and on the boundary conditions for the eigenwaves, which control the wave function shape near interfaces and surfaces.

3.4 Extended Drift Diffusion Model

A more complete model for carrier transport is based on the hydrodynamic equations derived from the Boltzmann transport equation, which takes into account energy and momentum relaxation effects [10]. Improved simulations can be achieved either by solving the hydrodynamic equations selfconsistently or by solving them under some simplifying assumption. One such approach yields a model for the carrier temperatures ($U_T = kT/q$) which depends only on local quantities [24].

$$U_{T\,n,p} = U_{To} + \frac{2}{3}\,\tau^{\epsilon}_{n,p}\,(v^{sat}_{n,p})^2 \left(\frac{1}{\mu^{LISE}_{n,p}} - \frac{1}{\mu^{LIS}_{n,p}}\right) \quad (15)$$

The energy relaxation times $\tau^{\epsilon}_{n,p}$ are in the order of 0.5 ps and just weakly temperature dependent [6]. The field degraded mobilities $\mu^{LISE}_{n,p}$ are modeled more accurately by using carrier specific driving forces instead of the simple electric field [24] (notation see [64]).

This local model for the carrier temperatures allows a first order treatment of hot carrier effects employing a drift diffusion based device simulator.

In more recent developments the use of fully nonlocal transport coefficients is attempted. These coefficients are in general functionals of the local distribution function [7]. Therefore in regions with large spatial inhomogeneity analytical models become inadequate. However, the Monte Carlo method is well suited to evaluate these coefficients using the following definitions for mobility and thermal voltage:

$$\mu = q\,\frac{|<\mathbf{v}>|}{|<\hbar\mathbf{k}\;\lambda_{\mathrm{m}}(\mathrm{E})>|}, \quad U_{T\,ij} = \frac{1}{q} <\hbar k_i\, v_j> \quad (16)$$

$<\mathbf{v}>$ is the average particle velocity and $\lambda_m(E)$ is the momentum scattering rate. The thermal voltage in its rigorous form has tensor property. Fig. 4 depicts the main diagonal temperatures in the area near the drain of a quarter micron MOSFET.

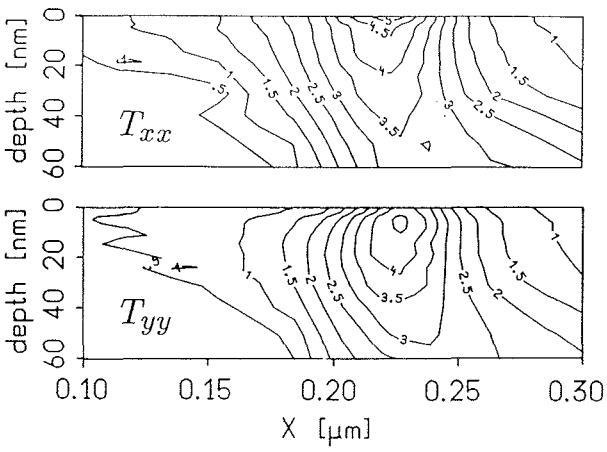

Fig. 4: Lateral (T_{xx}) and transversal (T_{yy}) electron temperatures in a quarter micron MOSFET (units 1000 K)

4 CONCLUSION

The preceding sections put particular emphasis on different details in the area of ULSI process and device simulation. To benefit from the rapid progress in modeling techniques coupling of the various modeling tools becomes more and more important. The increase in performance of new computer systems and networks aids this development. Integrated technology CAD environments make optimization of technology parameters feasible in an automate manner [31, 34, 37].

ACKNOWLEDGMENT

This work is considerably supported by the research laboratories of DIGITAL EQUIPMENT CORPORATION at Hudson, U.S.A., and the research laboratories of SIEMENS AG at Munich, FRG.

References

[1] S.T. Ahn et al., IEEE ED-37, 3 (1990) 806.
[2] M. Ali-Omar, L. Reggiani, SSE-30 (1987) 693.
[3] T. Ando et al., Rev.Mod.Phys. 54 (1982) 437.
[4] D.A. Antoniadis et al., J.Appl.Phys. 53 (1982) 6788.
[5] D.A. Antoniadis, in: Process and Device Simulation for MOS-VLSI Circuits, (Martinus Nijhoff, The Hague, 1983) pp. 1–47.
[6] G. Baccarani, M.R. Wordeman, SSE-28 (1985) 407.
[7] S. Bandyopadhyay et. al, IEEE ED-34 (1987) 392.
[8] G. Bastard, J.A. Brum, IEEE QE-22 (1986) 1625.
[9] J.P. Biersack, L.G. Haggmark, Nucl.Instr.Meth. 174 (1980) 257.
[10] K. Blotekjaer, IEEE ED-17 (1970) 38.
[11] G.B. Bronner, J.D. Plummer, J.Appl.Phys. 61 (1987) 5286.
[12] M. Budil et al., Mat.Sci.F., Vol.38-41 (1989) 719.
[13] T.L. Chiu, H.N. Ghosh, IBM J.Res.Dev. 15 (1971) 472.
[14] B.E. Deal, A.S. Grove, J.Appl.Phys. 36 (1965) 3770.
[15] P. Fahey et al., Appl.Phys.Lett. 46 (1984) 784.
[16] R.B. Fair, J.C.C. Tsai, J.Elect.Chem.Soc. 124 (1977) 1107.
[17] R.B. Fair, in: Impurity Doping Processes in Silicon, (North-Holland, Amsterdam, 1981) pp. 315–442.
[18] W. Fawcett et. al., J.Phys.Chem.Sol. 31 (1970) 1963.
[19] S. Furukawa et al., Jap.J.Appl.Phys. 11, (1972) 134.
[20] J.F. Gibbons et al., Projected Range Statistics (Halstead Press, Strandsberg, 1975).
[21] M.D. Giles, IEEE CAD-5 (1986) 679.
[22] E. Guerrero et al., J.Elect.Chem.Soc. 129 (1982) 1826.
[23] H. K. Gummel, IEEE ED-11 (1964) 455.
[24] W. Hänsch, S. Selberherr, IEEE ED-34 (1987) 1074.
[25] G. Hobler, S. Selberherr, IEEE CAD-7 (1988) 174.
[26] G. Hobler, NASECODE VI (1989) 501.
[27] G. Hobler et al., ESSDERC-90 (1990), in print.
[28] G. Hobler et al., NUPAD-3 (1990) 13.
[29] E.A. Irene, J.Appl.Phys. 54 (1983) 5416.
[30] C. Jacoboni, L. Reggiani, Rev.Mod.Phys. 55 (1983) 645.
[31] H. Jacobs et. al., NUPAD-3 (1990) 55.
[32] W. Jüngling et al. IEEE SC-20 (1985) 76.
[33] D.B. Kao et al., IEEE ED-35 (1988) 25.
[34] K. Kato et.al, IEEE ED-34, 10 (1987) 2049.
[35] M. Law, NUPAD-3 (1990) 9.
[36] U. Littmark, J.F. Ziegler, IBM Rep. 34401, (San Jose, 1979).
[37] P. Lloyd et. al., SISDEP-3 (1988) 111.
[38] A.M. Mazzone, G. Rocca, IEEE CAD-3 (1984) 64.
[39] A.M. Mazzone, Appl.Phys.A 45 (1988) 113.
[40] A.E. Michel et al., Appl.Phys.Lett. 51 (1987) 487.
[41] S. Mizuo, H. Higuchi, Jap.J.Appl.Phys. 21 (1982) pp. 56–60, pp. 272–275, pp. 281–286.
[42] N.F. Mott et al., Phil.Mag.B 60 (1989) 189.
[43] B.J. Mulvaney, W.B. Richardson, Appl.Phys.Lett. 51 (1987) 1439.
[44] B.J. Mulvaney et al., IEEE CAD-8 (1989) 336.
[45] E.H. Nicollian, A. Reisman, J.Elect.Mat. 17 (1988) 263.
[46] O.S. Oen, M.T. Robinson, Nucl.Instr.Meth. 132 (1976) 641.
[47] M. Orlowski, Appl.Phys.Lett. 53 (1988) 1439.
[48] W.A. Orr Arrienzo et al., J.Appl.Phys. 63 (1988) 116.
[49] B.R. Penumalli, IEEE ED-30 (1983) 986.
[50] A. Phillips, P.J.Price, Appl.Phys.Lett. 30 (1977) 528.
[51] P. Pichler, R. Ryssel, AEÜ El. and Comm. 44 (S.Hirzel, Stuttgart, 1990) 172.
[52] J.D. Plummer, B.E. Deal, in: Process and Device Simulation for MOS-VLSI Circuits, (Martinus Nijhoff, The Hague, 1983) pp. 48-87.
[53] C.S. Rafferty, ESSDERC-90 (1990), in print.
[54] H. D. Rees, Phys.Lett.A 26 (1968) 416.
[55] H. D. Rees, J.Phys.Chem.Sol. 30 (1969) 643.
[56] H. Runge, Phys.Stat.Sol.A 39 (1977) 595.
[57] H. Ryssel et al., Appl.Phys.Lett. 24 (1981) 39.
[58] H. Ryssel et al., Appl.Phys.A 41 (1986) 201.
[59] H. Ryssel, J.P. Biersack, in: Process and Device Modeling, (Elsevier Science, 1986) pp.31–69.
[60] N. Saito et al., IEDM-89 (1989) 625.
[61] E. Sangiorgi, B. Ricco IEEE CAD-7, (1988) 259.
[62] E. van Schie, J. Middlehoek, IEEE CAD-8 (1989) 108.
[63] A. Seidl et al., SISDEP-88 (1988) 277.
[64] S. Selberherr, Analysis and Simulation of Semiconductor Devices (Springer, Wien New York, 1984)
[65] S. Selberherr et al., AEÜ El. and Comm. 44 (S.Hirzel, Stuttgart, 1990) 161.
[66] W. Shockley, J.T. Last, Phys.Rev. 107 (1957) 392.
[67] F. Stern, S. Das Sarma, Phys.Rev.B 30 (1984) 840.
[68] J.L. Stone, J.C. Plunkett, in: Impurity Doping Processes in Silicon, (North-Holland, Amsterdam, 1981) pp.56–146.
[69] P. Sutardja, W.G. Oldham, IEEE ED-36 (1989) 2415.
[70] T. Takeda, A. Yoshii, IEEE EDL-6 (1985) 323.
[71] T.Y. Tan, U.Gösele, Appl.Phys.A 37 (1985) 1.
[72] K. Taniguchi et al., Appl.Phys.Lett. 42 (1983) 961.
[73] W.A. Tiller, J.Elect.Chem.Soc. 127 (1980) 619.
[74] J.R. Troxell, SSE-26 (1983) 539.
[75] M.Y. Tsai et al., J.Appl.Phys. 51 (1980) 3230.
[76] T. L. Tung et al., IEEE CAD-7 (1988) 215.
[77] H. Umimoto et al., IEEE CAD-8 (1989) 599.
[78] G.D. Watkins, in: Lattice Defects in Semiconductors, Vol.Inst.Phys.Conf.Ser.No.23, 1975.
[79] K.B. Winterbon, Ion Implantation and Energy Deposition, Vol. 2, (IFI Plenum, New York, 1975).
[80] D.R. Wolters et al., J.Appl.Phys. 65 (1989) 5126.
[81] J. Yoshida, IEEE ED-33, (1986) 154.